Design Space Exploration and Performance Analysis of Low Temperature PEM Fuel Cell Propulsion Aircraft

Yi-Chih Wang,
Swapnil Sarjerao Jagtap
Department of Aerospace Engineering
University of Michigan
Ann Arbor, Michigan, USA
ycwangd@umich.edu;
swapnilj@umich.edu

Blake Moffitt,
Jennifer Hallbach
Sikorsky
a Lockheed Martin Company
Connecticut, USA
blake.a.moffitt@lmco.com;
jennifer.e.hallbach.i@lmco.com

Gokcin Cinar
Department of Aerospace Engineering
University of Michigan
Ann Arbor, Michigan, USA
cinar@umich.edu
Corresponding author

Abstract—Hydrogen propulsion using low-temperature proton exchange membrane fuel cells (LT-PEMFC) offers a promising alternative to conventional combustion engines by reducing component complexity, lowering operating temperatures, and potentially decreasing operating costs. This paper presents a comprehensive system-level analysis of hydrogen-powered LT-PEMFC propulsion systems for aircraft. Custom-developed models integrate fuel cells with auxiliary subsystems, including thermal management, compression, and power electronics, to size the propulsion system and fuel capacity according to a defined mission profile. Key performance metrics, including range, endurance, and liquid hydrogen volume requirements, are evaluated for a generic general aviation class baseline aircraft sized with an automotive-derived net 150 kW LT-PEMFCs. The analysis considers six key design variables (gross takeoff weight (GTOW), lift-to-drag ratio, propulsion efficiency, propulsion specific power, liquid hydrogen gravimetric index, and GTOW mass fraction) along with three operational parameters (climb rate, service ceiling, and cruise speed). Validation against an established flight mission demonstrates close agreement in liquid hydrogen consumption predictions. Under baseline operational conditions, the aircraft with a 1,814 kg GTOW is predicted to achieve a range of 3,203 km and 17.5 hours of flight. Sensitivity analyses indicate that when subjected to alternative design and operational constraints, incremental improvements in the GTOW mass fraction enable an additional 100 km of range with a minimal adjustment, while enhancements in the lift-to-drag ratio and propulsion efficiency reduce the liquid hydrogen required by 64% and 50% per 100 km relative to other design variables, respectively. Advanced technology improvements suggest a maximum performance potential of 15,474 km in range and 84.7 hours of flight time. These findings provide critical insights for optimizing fuel cell propulsion systems and establishing a clean-sheet design framework for next-generation hydrogen-powered aircraft.

Index Terms—low-temperature proton exchange membrane, fuel cells, system integration, liquid hydrogen, aircraft design, sensitivity analysis.

I. Introduction

This research investigates the potential of hydrogen and low-temperature proton exchange membrane fuel cells (LT-PEMFCs) as energy sources for new-generation aircraft propulsion. Hydrogen offers a higher gravimetric energy density (120 MJ/kg) compared to conventional jet fuel (36 MJ/kg) and lithium-ion (Li-ion) batteries (1 MJ/kg). Additionally, it enables rapid refueling times ranging from 3 to 5 minutes (gaseous hydrogen) to run 646 km, close to conventional vehicle [1]–[3]. Fuel cells with hydrogen tanks, compared to Li-ion batteries, provide superior energy density and extended operational lifespans [4]. According to the U.S. Department of Energy, fuel cell stacks for on-the-ground vehicles can achieve a service life of up to 321,868 km, significantly outperforming Li-ion batteries, rated for approximately 160,934 km [5]. Furthermore, fuel cells produce only water as an emission [6].

The research surveyed and collected data on the commercial LT-PEMFC products and applications that came to market between 2005 and 2025 at the stack and system level. Fig. 1 illustrates the gravimetric specific power progress of commercial LT-PEMFC products and systems over the past two decades [7]–[16]. The stack-specific power of LT-PEMFCs has improved substantially from 0.5 kW/kg to 3 kW/kg over 20 years. However, the overall system-specific power remains constrained at approximately 0.8 kW/kg, primarily due to the substantial weight of the thermal management system required to maintain membrane humidity in LT-PEMFCs.

Additionally, hydrogen as a fuel for fuel cells can be stored in various forms, including as a pure gas, a pure liquid, or a solid where hydrogen is chemically bonded to other molecules. For the majority of aviation applications, hydrogen is typically stored either as a liquid (LH2) or as a compressed gas (CGH2) [17]. LH2 offers a higher volumetric energy density of 8.5 MJ/L and a gravimetric fraction ranging from 30% to 90%, compared to CGH2, which provides 2.9 to 4.8 MJ/L and 1% to 15%, respectively [18], [19]. These values are illustrated in
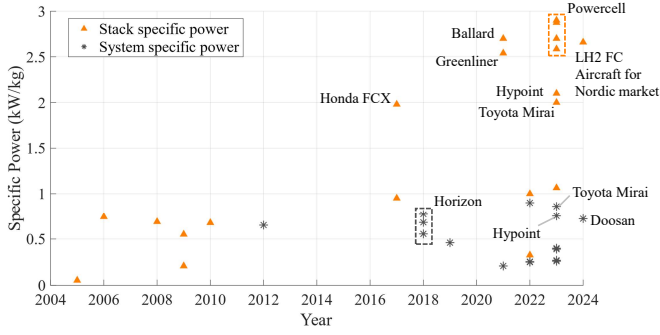
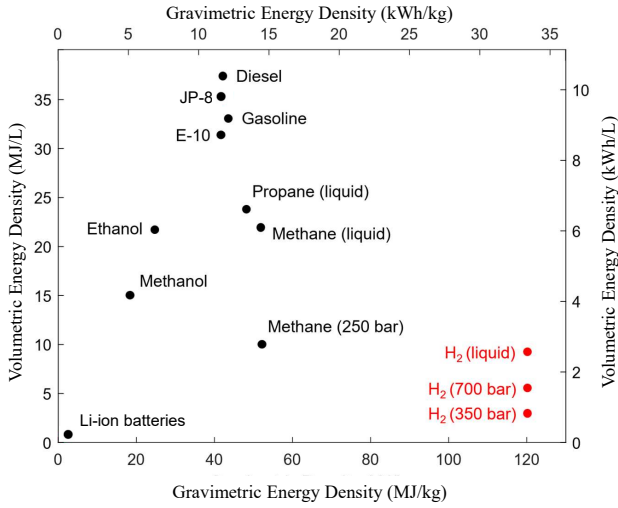Fig. 1. The stack and system specific power of commerical LT-PEMFC products and systems in past 20 years.

Fig. 2. The specific energy and energy density for several fuel types [20].

Fig. 2. Consequently, LH2 is more advantageous for aviation purposes than CGH2, requiring less volume and weight to store an equivalent amount of energy.

While much research has focused on fuel cells and their subsystems like motors and converters [8], [21]–[25], there is a gap in integrating fuel cell systems and performing sensitivity analyses on aircraft performance. Most developments have focused on improving the fuel cell system without addressing how sensitive overall performance is to design parameters related to the aircraft, which may affect vehicle performance. This study aims to address this gap by integrating the components and identifying key factors that influence aircraft performance, ultimately contributing to the development of a clean-sheet design for hydrogen fuel cell-powered aircraft.

II. TECHNICAL APPROACH

In this research, the aircraft design, fuel cell propulsion system, and flight mission analysis are modeled using MAT-LAB. The fuel cell propulsion system and fuel capacity are sized based on the maximum power requirements of the design mission. Six design variables are evaluated: (1) gross takeoff weight (GTOW), (2) lift-to-drag ratio (L/D), (3) propulsion system efficiency, (4) propulsion system specific power, (5)

LH2 gravimetric index, and (6) GTOW mass fraction. LH2 gravimetric index is the ratio of the mass of stored LH2 to the total mass of the tank, including LH2. The GTOW mass fraction is the ratio of the mass of aircraft excluding payload, propulsion system, and fuel to GTOW. Additionally, three operational conditions are considered: (1) climb rate, (2) service ceiling, and (3) cruise speed, which influence the aircraft's power demand and fuel capacity requirements.

This study evaluates aircraft performance under a range of technology options, design configurations, and operational scenarios. It employs sensitivity and trade-off analyses to identify the key factors that influence the range and endurance of the aircraft.

A. Low Temperature Proton Exchange Membrane Fuel Cells

LT-PEMFCs generate electricity through the electrochemical reaction of hydrogen and oxygen. In this process, the chemical energy of the fuel is converted into electricity and exhaust heat. The electricity produced is delivered to external electrical loads through circuits, while the exhaust heat is released into the surrounding environment. Considering electrochemical principles, thermodynamics, and potential losses during operations—such as activation loss, ohmic loss, and concentration loss—the actual potential output is given by (1) [26].

$$U = E_{\text{Nernst}} - E_{\text{act}} - E_{\text{ohm}} - E_{\text{con}} \tag{1}$$

where U, E_{Nernst}, E_{act}, E_{ohm} and E_{con} are the actual potential, Nernst potential, the activation loss, the ohmic loss and the concentration loss. According to electrochemical and thermodynamic principles, when no external electrical load is applied, the highest reversible voltage of a single LT-PEMFC, E_{Nernst}, can be determined using the Nernst equation [27] in (2).

$$E_{\text{Nernst}} = E^{\circ} + \frac{\Delta S}{n_e F}(T - T_0) + \frac{RT}{n_e F}\ln\left(\frac{p_{H_2}p_{O_2}^{0.5}}{p_{H_2O}}\right) \tag{2}$$

where E° is the ideal standard reference potential (298.15 K and 1 atm) which is 1.229 V for liquid water; $\Delta S = -164.25\ Jmol^{-1}K^{-1}$ is the entropy change to generate liquid water; $n_e = 2$ is the number of electrons exchanged per hydrogen molecule; F is the Faraday's constant; T and T_0 are the temperature of LT-PEMFC and the ambient; R is the ideal gas constant and p_{H_2}, p_{O_2} and p_{H_2O} are the partial pressure of hydrogen, oxygen and water (in atm), respectively.

The theoretical hydrogen consumption rate, $\dot{q}_{H_2}$ (kg/s) of LT-PEMFCs is shown in (3) [28], [29], where j is current density, A_0 is reaction area of single cell, N_{cell} is the number of cells.

$$\dot{q}_{H_2} = 1.05 \times 10^{-8} \times jA_0 \times N_{cell} \tag{3}$$

B. Propulsion Architecture

The designed propulsion system (single propulsor), as shown in Fig. 3, uses LT-PEMFCs as the primary power source and LH2 as the fuel. The electricity generated by the fuel cells is distributed through a power bus to support various systems: 15% of the total generated power is used to operate the compression and cooling systems for the fuel cells [30], [31],
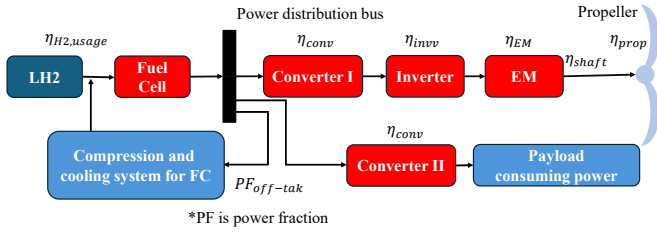
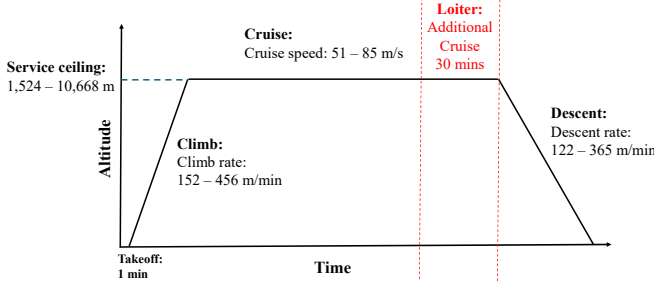Fig. 3. Single LT-PEMFC propulsion system configuration.

Fig. 4. Design mission profile.

around 10 kW is supplied as electrical power for the aircraft, and the remaining power drives the electric motor (EM) that propels the aircraft's propeller. Before powering the EM, the electricity must be converted and stabilized due to voltage fluctuations caused by the uniform fuel distribution required for the fuel cells' electrochemical reaction. Converters are applied to convert DC power into AC, as most high-efficiency motors, such as permanent magnet synchronous motors, are AC-based [32]. The direct-drive electric motor is connected to the propeller via a shaft, generating thrust for the aircraft.

C. Flight Mission Profile

The design mission in this research consists of the following segments: Takeoff, Climb, Cruise, Loiter, and Descent, which is a generic flight profile relative to manned aircraft, but also applicable to some unmanned aircraft system missions as well. During takeoff, the aircraft accelerates to the required speed to take off at full throttle within one minute. In the climb phase, the aircraft continues to accelerate until it reaches the designated cruise speed at the top of climb. The climb time is calculated based on the design climb rate and the service ceiling. In the cruise phase, the aircraft maintains a constant speed and altitude. For safety concerns, the aircraft must carry enough fuel for an additional 30-minute of the loiter phase as a reserve. Finally, the aircraft begins its descent at 80% of the climb rate. The range and endurance of the aircraft depend on whether there is sufficient fuel to complete takeoff, climb, the 30-minute loiter, and descent, under varying design and operational conditions.

D. Power Requirement Estimation

The power requirements for the flight mission are analyzed based on the law of conservation of energy. The power supplied by the fuel cells must match the power needed to overcome drag and changes in the aircraft speed and altitude, scaled by the relevant efficiency losses. Thus, P_{req}, at each point in the mission can be determined using (4) [33]:

$$P_{req} = TV = DV + \left(mg\frac{dh}{dt} + mV\frac{dV}{dt} \right) \quad (4)$$

where T is thrust; V is the aircraft speed; D is the drag of the aircraft; m is the aircraft mass; g is the gravitational acceleration; h is the altitude; dh/dt and dV/dt are the climb rate and acceleration of the aircraft, respectively; P_{req} is the power required to fly the mission.

The power output of fuel cells ($P_{FC,out}$) depends on P_{req}, the efficiencies of the propeller (η_{prop}), shaft (η_{shaft}), electric motor (η_{EM}), inverter (η_{Inv}), and converters (η_{Conv}), and the power fraction consumed by the compression and cooling systems ($PF_{off-take}$) [8], [22], [34]. Accordingly, the power output of the fuel cells can be expressed in (5)

$$P_{FC,out} = \frac{P_{req}}{\eta_{prop}\ \eta_{shaft}\ \eta_{EM}\ \eta_{Inv}\ \eta_{Conv}\ (1 - PF_{off-take})} \quad (5)$$

III. AIRCRAFT WEIGHT BREAKDOWN

This aircraft design integrates three main systems: aircraft, propulsion, and fuel system, with GTOW as their sum. The aircraft system is GTOW multiplied by GTOW mass fraction. Propulsion system weight is derived in two steps: first, specific power is calculated from a 150 kW Powercell Pstack and advanced subsystems [8], [22], [34]; second, it's sized by required power and specific power, including fuel cells, compression, thermal management, control, humidifier, motor, converters, inverter, propeller, and shaft. The fuel system, comprising a cryogenic tank and LH2, depends on the tank's gravimetric index. Payload fully supports the fuel system. GTOW composition is given by (6).

$$GTOW = GTOW \times m_{f,GTOW} + \frac{P_{req}}{SP_{prop}} + \frac{W_{LH2}}{m_{f,LH2}} \quad (6)$$

where $m_{f,GTOW}$ represents the GTOW mass fraction, SP_{prop} represents the specific power of the propulsion system (kW/kg), W_{LH2} represents the weight of stored LH2 (kg), and $m_{f,LH2}$ represent the gravimetric index of LH2 tank.

IV. RESULTS AND DISCUSSIONS

A. LT-PEMFC modeling and model validation

This research examines various LT-PEMFC technologies by modeling their polarization curves (shown in Fig. 5) to evaluate performance characteristics. The Powercell Pstack product tested at 100 kPa [12] serves as the baseline technology, referred to as the *"Baseline"* scenario. The "Ref. c" in Fig. 5 [35] represents the state-of-the-art LT-PEMFC technology, referred to as the *"State-of-the-Art: 2024"* scenario. Additionally, a future performance target, termed *"Future (Powercell 4 A/cm²)"*, is proposed, representing an estimated improvement over the current Powercell product based on potential technological advancements. For sensitivity analysis, these
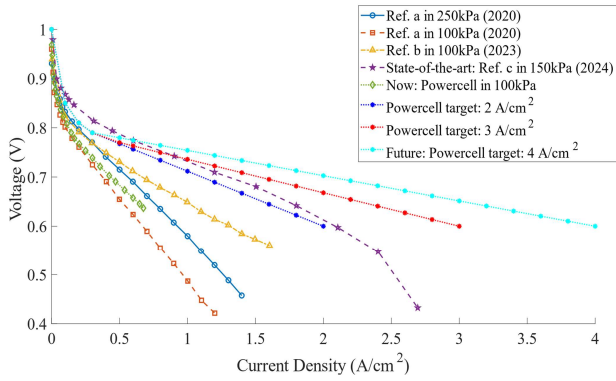
Fig. 5. The polarization curves of different LT-PEMFC designs.

Variable	Boundary	Baseline	Unit
GTOW	$907 - 5{,}216$	1,814	kg
L/D ratio	$18 - 22$	18	-
Propulsion efficiency	$0.646 - 0.8$	0.646	-
Propulsion specific power	$0.494 - 0.615$	0.494	kg/kW
LH2 gravimetric index	$0.4 - 0.6$	0.4	-
GTOW mass fraction	$0.7 - 0.6$	0.7	-
Climb rate	$152 - 456$	152	m/min
Service ceiling	$1{,}524 - 10{,}668$	1,524	m
Cruise speed	$51 - 85$	51	m/s

Case	GTOW (kg)	Propulsion system weight (kg)	LH2 weight (kg)	Range (km)	Endurance (hr)
I	907	159.6	44.9	2,670	14.6
II	1,814	301.0	96.8	3,203	17.5
III	2,948	479.7	161.7	3,465	19
IV	5,216	835.4	291.6	3,680	20.1

three polarization curves are selected. When these fuel cell designs are integrated with all subsystems—including thermal management, compression, electrical components, and propulsion components [8], [12], [22], [34]—the specific power of the propulsion system is calculated to be 0.494 kW/kg, 0.557 kW/kg, and 0.615 kW/kg, respectively, indicating a trend of increasing efficiency and reduced weight.

To validate the accuracy of this technical approach, fuel consumption is modeled using the specifications and mission profile of Joby Aviation's SHy4 hydrogen-electric aircraft. The SHy4 completed a flight of 847 km over 4.8 hours, consuming 36 kg of LH2, while cruising at an altitude of approximately 274 m with a lift-to-drag (L/D) ratio of 12.5 and a maximum takeoff weight of 2,404 kg [36], [37]. In our MATLAB-based simulation, the LH2 consumption is estimated at 35.5 kg—a deviation of -1.4% from the actual value. This close alignment suggests that the proposed modeling method can provide reliable and reasonable estimations.

B. Sensitivity analysis of design and operational variables

The baseline design, operational conditions, and design space boundaries for fixed-wing aircraft are defined in Table I. A constant payload power consumption of 10 kW is assumed for the entire mission duration. The lower bounds reflect current technological feasibility, while the upper bounds for GTOW, climb rate, service ceiling, and cruise speed correspond to publicly available specifications for the MQ-9 Reaper [38], [39]. Upper bounds for propulsion efficiency and specific power reflect projections for future technologies and state-of-the-art electric components.

The baseline configuration corresponds to a high-aspect-ratio, efficient aircraft constructed from conventional materials, akin to designs typical of general aviation and unmanned aerial vehicles. Using parameters from Table I, aircraft performance is evaluated across GTOW scenarios listed in Table II, specifically: (I) 907 kg (comparable to a Trainer Diamond DA40 XLT), (II) 1,814 kg (baseline) (III) 2,948 kg (similar to a Cessna Caravan), and (IV) 5,216 kg (similar to an MQ-9 Reaper). The propulsion system is sized based on maximum power required during the mission.

Results indicate marginal benefits in range and endurance with increased LH2 capacity, shown as an aggregate increase in GTOW under baseline design conditions. Higher GTOW corresponds to higher LH2 storage but heavier operation empty weight and faster fuel consumption due to higher power demand, offsetting the benefit of increased LH2 storage. Specifically, moving from Case I to Case II, each additional 100 kg of GTOW adds 58 km of range and 0.3 hours of endurance. However, from Case I to Case III, each additional 100 kg of GTOW results in smaller gains of 38 km in range and 0.2 hours in endurance. This diminishing return occurs because although a baseline aircraft with higher GTOW provides higher LH2 capacity, it also elevates power requirements, increasing fuel consumption and limiting net benefits.

Fig. 6 illustrates aircraft performance under varying operational conditions: service ceiling, climb rate, and cruise speed. Blank regions in the plots expand at higher cruise speeds and climb rates, indicating insufficient fuel capacity to complete the mission. Higher climb rates and cruise speeds require greater power from the fuel cells, necessitating a heavier propulsion system. This added weight reduces available LH2 storage capacity and accelerates fuel consumption, rendering certain design points infeasible.

Continuing with Fig. 6, doubling the climb rate from 152 to 304 m/min at a baseline service ceiling of 6,000 m reduces the range from 3,245 km to 1,615 km (-50%). Increasing cruise speed from 51 m/s to 85 m/s (+66%) at a fixed climb rate of 152 m/min reduces range to 1,694 km (-48%). These results underscore the trade-off between higher propulsion demands and available LH2 storage. In contrast, higher GTOW under baseline conditions provides additional fuel storage capacity, thus compensating for the elevated power demands due to higher cruise speeds.
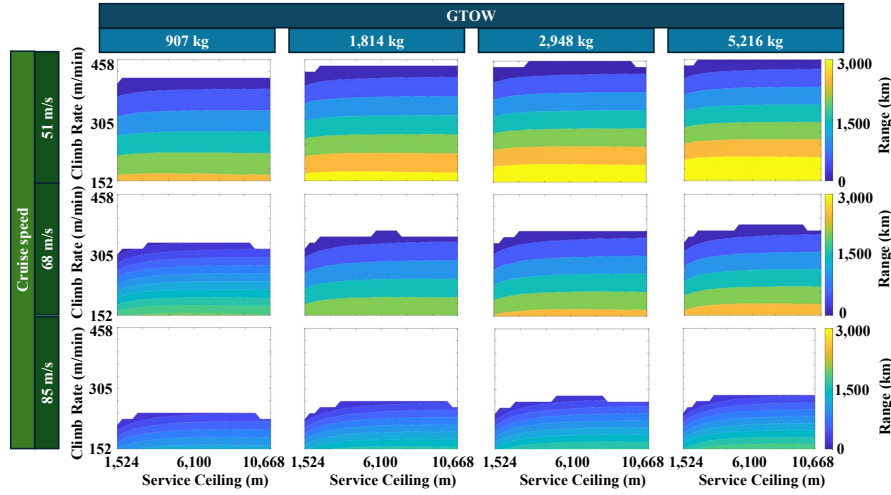
Fig. 6. The range estimation of the aircraft with different operational variables and GTOW.

Fig. 6 also shows negligible (∼1%) effect on range and endurance when increasing the service ceiling from 1,524 m to 6,000 m at lower cruise speeds, as propulsion system sizing and LH2 storage requirements remain similar. However, at higher cruise speeds attained at the top of climb, lowering the ceiling from 6,000 m to 1,524 m demands additional climb power to achieve the required kinetic energy (i.e., heavier propulsion system at the same GTOW), thus reducing available LH2 storage capacity. For example, for a baseline aircraft at 85 m/s cruise speed, a lower ceiling reduces range by 20% and endurance by 25%.

Thus, under baseline conditions, maximizing aircraft range involves balancing climb rate, cruise speed, and service ceiling relative to LH2 capacity. To maximize range, lower climb rates and cruise speeds are optimal. Higher climb rates and cruise speeds should be coupled with increased service ceilings to minimize power demand and maintain LH2 capacity.

Table III summarizes the sensitivity analysis of key design variables impacting aircraft range (R), endurance (t), and required LH2 volume in liters (L). Two evaluation approaches are applied: (i) performance improvements within predefined design constraints and (ii) incremental improvements required for an additional 100 km of range under design variable boundaries. The first approach identifies GTOW mass fraction as most beneficial, whereas specific power of the propulsion system (related to fuel cell technology) has the least impact due to limited improvement potential. However, different boundaries limit the fairness of comparisons.

The second approach in Table IV standardizes comparisons by quantifying LH2 volume needed for an additional 100 km from baseline. Improvements in L/D ratio and propulsion efficiency require significantly less LH2 (13.67 L and 18.81 L, respectively) compared to GTOW mass fraction (38 L), representing reductions of approximately 64% and 50%. These reductions stem from reduced power demands, enabling a lighter propulsion system and freeing capacity for LH2 storage, thus maintaining range with minimal LH2 increases. Conversely,

TABLE III
PERFORMANCE ESTIMATION OF HYDROGEN LT-PEMFC AIRCRAFT WITH GTOW = 1,814 KG AND BASELINE OPERATIONAL SETTINGS (RANGE = 3,203 KM, ENDURANCE = 17.5 HR AND LH2 VOLUME = 1,369 L).

	L/D ratio	GTOW mass fraction	LH2 gravi. index	Propulsion system efficiency	Propulsion specific power
Improve (from→to)	18 → 22	0.7 → 0.6	0.4 → 0.6	0.646 → 0.8	0.494 → 0.615
ΔR (km)	+1,217 (+38%)	+2,690 (+84%)	+1,825 (+57%)	+1,633 (+51%)	+630 (+20%)
Δt (hr)	+6.3 (+36%)	+14.4 (+82%)	+9.6 (+55%)	+8.9 (+51%)	+3.4 (+19%)
ΔLH2 (L)	+164 (+12%)	+1,026 (+75%)	+684 (+50%)	+301 (+22%)	+336 (+24%)

TABLE IV
DESIGN VARIABLE IMPROVEMENT OF HYDROGEN LT-PEMFC AIRCRAFT FOR EACH ADDITIONAL 100 KM FROM BASELINE SETTINGS.

Incremental Changes per +100 km from baseline:					
	ΔL/D ratio	ΔGTOW mass fraction	ΔLH2 gravi. index	ΔPropulsion system efficiency	ΔPropulsion specific power
Value/100 km	+0.33	-0.004	+0.01	+0.009	+0.019
Δt (hr/100 km)	+0.53	+0.53	+0.53	+0.56	+0.54
ΔLH2 (L/100 km)	+13.67	+38	+38	+18.81	+53.33

improvements in GTOW mass fraction and LH2 gravimetric index directly increase storage capacity but require greater LH2 volume (38 L) to achieve additional 100 km of range as power demands remain unchanged.

Increasing specific power of the propulsion system enables weight savings, which can be allocated to extra LH2 storage capacity. However, actual gains depend on the performance of the LT-PEMFCs. In this paper, three LT-PEMFC technologies (Fig. 5, modeled based on [12], [35]) with different voltages and current densities at peak power conditions were ana-
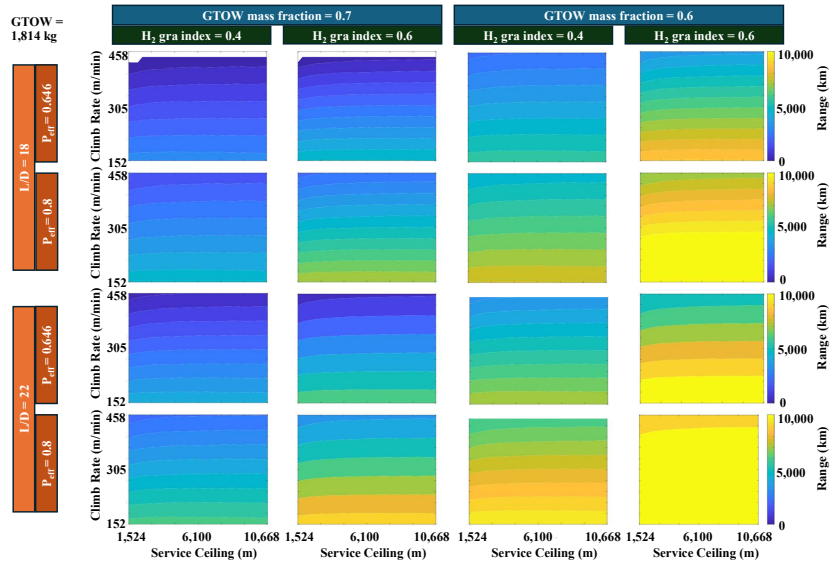
Fig. 7. Performance matrix of the aircraft with 1,814 kg of GTOW based on multi design variable changes.

lyzed. Although future LT-PEMFC technologies offer higher specific power, their lower voltage at peak load increases fuel consumption, partially offsetting weight savings. Further improvements depend significantly on reducing the thermal management system mass, which, in this paper, is assumed to have a specific power of around 0.7 kW/kg, accounting for over 60% of the fuel cell propulsion system mass.

Fig. 7 provides a performance matrix for a 1,814 kg GTOW aircraft, analyzing the global sensitivity of design and operational variables. With a fixed L/D ratio and varying LH2 propulsion assumptions, the results under baseline operational settings show that GTOW mass fraction paired with LH2 gravimetric index boosts range by +179%, more than the GTOW mass fraction with propulsion efficiency (+148%), or LH2 gravimetric index with propulsion efficiency (+130%), due to having higher LH2 capacity. Despite having improved aerodynamic design (L/D ratio), GTOW mass fraction remains critical in impacting LH2 storage capacity and range. For example, if we only consider the combination of L/D ratio with propulsion efficiency and LH2 gravimetric index, the range will increase +93% and +106%, lower than 179%. Optimizing both power-reducing factors (L/D, propulsion efficiency) and storage-enhancing variables (GTOW mass fraction, LH2 gravimetric index) simultaneously yields substantial performance gains–up to a 380% (15,474 km) increase in range–highlighting the importance of integrated optimization for maximum aircraft performance.

V. CONCLUSION

This research presented a comprehensive system-level sensitivity analysis of hydrogen LT-PEMFC propulsion for aircraft. Custom-developed models were used to evaluate the impact of six design variables and three operational parameters on critical performance metrics such as range, flight duration, and LH2 requirements. The analysis reveals that a higher

GTOW with increased LH2 storage capacity can compensate for the higher fuel consumption associated with increased aircraft weight, thereby enabling greater range and endurance capabilities. Furthermore, improvements in aerodynamic efficiency (L/D ratio) and propulsion system efficiency effectively reduce power requirements, while enhancements in GTOW mass fraction (i.e., lower values) and LH2 gravimetric index substantially increase LH2 storage. In combination, reducing power demand and enhancing LH2 storage significantly boost aircraft performance, with the GTOW mass fraction proving particularly influential in increasing LH2 storage capacity. In contrast, improvements in specific power of the propulsion system have limited effects on overall performance due to the significant weight of the thermal management system.

Operationally, higher cruise speeds and climb rates reduce range and endurance by increasing power demand and propulsion system weight, which in turn increases fuel consumption and limits LH2 storage capacity. At lower speeds and climb rates, the service ceiling has a relatively minor impact on range and endurance. However, under high cruise speed and climb rate conditions, a higher service ceiling can enhance performance by lowering power requirements, easing climb acceleration demands, and allowing for a less powerful and hence lighter propulsion system and greater LH2 capacity.

For optimal aircraft design, investment should be prioritized in reducing the GTOW mass fraction (like reducing the airframe and other operational empty weights) to free additional capacity for LH2 storage. Even modest improvements in this area yield significant increases in storage capacity, thereby extending both range and endurance. When combined with enhancements to the L/D ratio or propulsion system efficiency, this approach reduces the fuel consumption and increases LH2 storage, delivering substantial performance benefits.

Future work should focus on quantifying the cost and feasibility of improving these design variables, exploring

hybrid electrified configurations, and further optimizing fuel consumption for specific mission profiles to refine the design framework for next-generation hydrogen-powered aircraft.

VI. Acknowledgment

References

[1] S. Gupta and R. Perveen, "Fuel cell in electric vehicle," *Materials Today: Proceedings*, vol. 79, pp. 434–437, 2023, international Conference on Startup ventures: Technology Developments and Future Strategies.

[2] C. L. Pastra, G. Cinar, and D. N. Mavris, "Feasibility and benefit assessments of hybrid hydrogen fuel cell and battery configurations on a regional turboprop aircraft," in *AIAA AVIATION 2022 Forum*, 2022, p. 3290.

[3] Toyota Motor Corporation. (2025) Mirai. Toyota Motor Corporation. Last accessed: March 18, 2025. [Online]. Available: https://www.toyota.com/mirai/

[4] D. De Wolf and Y. Smeers, "Comparison of battery electric vehicles and fuel cell vehicles," *World Electric Vehicle Journal*, vol. 14, no. 9, 2023.

[5] U.S. Department of Energy. (2022) DOE Technical Targets for Fuel Cell Transit Buses. U.S. Department of Energy. Last accessed: March 25, 2025. [Online]. Available: https://www.energy.gov/eere/fuelcells/doe-technical-targets-fuel-cell-transit-buses

[6] T. Sousa, M. Mamlouk, and K. Scott, "An isothermal model of a laboratory intermediate temperature fuel cell using pbi doped phosphoric acid membranes," *Chemical Engineering Science*, vol. 65, no. 8, pp. 2513–2530, 2010.

[7] Ballard Power Systems. (2021) FCgen® - Fuel Cell Stacks. Ballard Power Systems. Last accessed: March 18, 2025. [Online]. Available: https://www.ballard.com/fcgen/

[8] M. Gosalvez, J. van Ham, S. Joosten, D. Juschus, G. Nieuwerth, T. Pelt, L. Smit, M. Takken, Y. Wang, T. Ziere, F. Leverone, P. Groen, and M. Delgado Schwartz, ""the greenliner", green flying final report dse group 8," 07 2018.

[9] Doosan Mobility Innovation. (2024) Powerpack. Doosan Mobility Innovation. Last accessed: March 18, 2025. [Online]. Available: https://www.doosanmobility.com/en/products/powerpack

[10] Horizon Fuel Cell Technologies. (2018) Fuel cell stacks. Horizon Fuel Cell Technologies. Last accessed: March 18, 2025. [Online]. Available: https://www.horizonfuelcell.com/fuel-cell

[11] Intelligent Energy. (2023) IE-DRIVE fuel cell systems. Intelligent Energy. Last accessed: March 18, 2025. [Online]. Available: https://www.intelligent-energy.com/our-products/ie-drive/

[12] PowerCell Group. (2022) Fuel cell stacks. PowerCell Group. Last accessed: March 18, 2025. [Online]. Available: https://powercellgroup.com/fuel-cell-stacks/

[13] Spectronik. (2022) Fuel cell. Spectronik. Last accessed: March 18, 2025. [Online]. Available: https://www.spectronik.com/fuel-cell

[14] C. Svensson, A. A. Oliveira, and T. Grönstedt, "Hydrogen fuel cell aircraft for the nordic market," *International Journal of Hydrogen Energy*, vol. 61, pp. 650–663, 2024.

[15] S. Tanaka, K. Nagumo, M. Yamamoto, H. Chiba, K. Yoshida, and R. Okano, "Fuel cell system for honda clarity fuel cell," *eTransportation*, vol. 3, p. 100046, 2020.

[16] Y. Wang, D. F. Ruiz Diaz, K. S. Chen, Z. Wang, and X. C. Adroher, "Materials, technological status, and fundamentals of pem fuel cells – a review," *Materials Today*, vol. 32, pp. 178–203, 2020.

[17] M. G. Sürer and H. T. Arat, "State of art of hydrogen usage as a fuel on aviation," *European Mechanical Science*, vol. 2, no. 1, pp. 20–30, 2018.

[18] E. J. Adler and J. R. Martins, "Hydrogen-powered aircraft: Fundamental concepts, key technologies, and environmental impacts," *Progress in Aerospace Sciences*, vol. 141, p. 100922, 2023.

[19] B. A. Moffitt, *A methodology for the validated design space exploration of fuel cell powered unmanned aerial vehicles*. Georgia Institute of Technology, 2010.

[20] Energy gov. (n.d.), "Hydrogen storage," 2020, last accessed: December 08, 2023. [Online]. Available: https://www.energy.gov/eere/fuelcells/hydrogen-storage

[21] P. Wheeler, T. S. Sirimanna, S. Bozhko, and K. S. Haran, "Electric/hybrid-electric aircraft propulsion systems," *Proceedings of the IEEE*, vol. 109, no. 6, pp. 1115–1127, 2021.

[22] C. Hall, C. L. Pastra, A. Burrell, J. Gladin, and D. N. Mavris, "Projecting power converter specific power through 2050 for aerospace applications," in *2022 IEEE Transportation Electrification Conference Expo (ITEC)*, 2022, pp. 760–765.

[23] Z. S. Spakovszky, Y. Chen, E. M. Greitzer, Z. C. Cordero, J. H. Lang, J. L. Kirtley, D. J. Perreault, H. N. Andersen, M. M. Qasim, D. G. Cuadrado, D. M. Otten, and M. Amato, "Technology demonstration of a megawatt-class integrated motor drive for aircraft propulsion," in *AIAA AVIATION 2023 Forum*, 2023.

[24] S. Thangavel, D. Mohanraj, T. Girijaprasanna, S. Raju, C. Dhanamjayulu, and S. M. Muyeen, "A comprehensive review on electric vehicle: Battery management system, charging station, traction motors," *IEEE Access*, vol. 11, pp. 20994–21019, 2023.

[25] S. Tiwari, M. J. Pekris, and J. J. Doherty, "A review of liquid hydrogen aircraft and propulsion technologies," *International Journal of Hydrogen Energy*, vol. 57, pp. 1174–1196, 2024.

[26] D. Cheddie and N. Munroe, "Mathematical model of a pemfc using a pbi membrane," *Energy Conversion and Management*, vol. 47, no. 11, pp. 1490–1504, 2006.

[27] K. Scott, S. Pilditch, and M. Mamlouk, "Modelling and experimental validation of a high temperature polymer electrolyte fuel cell," *Journal of Applied Electrochemistry*, vol. 37, pp. 1245–1259, 2007.

[28] Y.-C. Wang and G. Cinar, "Modeling and simulation of high temperature proton exchange membrane fuel cells in parallel hybrid electric turboprop aircraft with multi whale optimization algorithms," in *AIAA AVIATION FORUM AND ASCEND 2024*, 2024, p. 3829.

[29] M. Bayat and M. Özalp, "Effects of leak current density and doping level on energetic, exergetic and ecological performance of a high-temperature pem fuel cell," *International Journal of Hydrogen Energy*, vol. 48, no. 60, pp. 23212–23229, 2023, the 6th International Hydrogen Technologies Congress (IHTEC-2022).

[30] R. Tirnovan and S. Giurgea, "Efficiency improvement of a pemfc power source by optimization of the air management," *International Journal of Hydrogen Energy*, vol. 37, no. 9, pp. 7745–7756, 2012, 7th Petite Workshop on the Defect Chemical Nature of Energy Materials, 14-17 March 2011, Storaas, Kongsberg, Norway.

[31] HyPoint Inc., "Hypoint's turbo air-cooled ht-pem fuel cell," 2021, last accessed January 08 2025. [Online]. Available: https://docsend.com/view/t9aw2mk

[32] I. López, E. Ibarra, A. Matallana, J. Andreu, and I. Kortabarria, "Next generation electric drives for hev/ev propulsion systems: Technology, trends and challenges," *Renewable and Sustainable Energy Reviews*, vol. 114, p. 109336, 2019.

[33] G. Cinar, "A methodology for dynamic sizing of electric power generation and distribution architectures." Georgia Institute of Technology, 2018.

[34] YASA Limited. (2025) Technology. YASA Limited. Last accessed: March 25, 2025. [Online]. Available: https://yasa.com/technology/

[35] T. Yin, D. Chen, T. Hu, S. Hu, R. Li, T. Wei, Y. Li, Y. Li, X. Xu, and P. Pei, "Experimental investigation and comprehensive analysis of performance and membrane electrode assembly parameters for proton exchange membrane fuel cell at high operating temperature," *Energy Conversion and Management*, vol. 315, p. 118740, 2024.

[36] Joby Aviation, Inc. (2024, Jul.) Joby demonstrates potential for regional journeys with landmark hydrogen-electric flight. Joby Aviation, Inc. Last accessed: March 18, 2025. [Online]. Available: https://www.jobyaviation.com/news/joby-demonstrates-potential-regional-journeys-landmark-hydrogen-electric-flight/

[37] A. Jha, N. Prabhakar, D. Karbowski, and B. German, "Urban air mobility: A preliminary case study for chicago and atlanta," in *2022 IEEE Transportation Electrification Conference Expo (ITEC)*, 2022, pp. 300–306.

[38] G. Cinar, A. A. Markov, J. C. Gladin, E. Garcia, D. N. Mavris, and S. S. Patnaik, "Feasibility assessments of a hybrid turboelectric medium altitude long endurance unmanned aerial vehicle," in *2020 AIAA/IEEE Electric Aircraft Technologies Symposium (EATS)*, 2020, pp. 1–17.

[39] U.S. Air Force. (2025) MQ-9 Reaper. U.S. Air Force. Last accessed: March 25, 2025. [Online]. Available: https://www.af.mil/About-Us/Fact-Sheets/Display/Article/104470/mq-9-reaper/